Available online at www.sciencedirect.com

ScienceDirect

Journal of the European Ceramic Society 30 (2010) 1021–1026

www.elsevier.com/locate/jeurceramsoc

Flexural strength and fracture behavior of ZrB_2–SiC ultra-high temperature ceramic composites at 1800 °C

Ping Hu*, Zhi Wang

Center for Composite Materials, Harbin Institute of Technology, Harbin 150001, PR China

Received 2 June 2009; received in revised form 13 September 2009; accepted 28 September 2009
Available online 24 October 2009

Abstract

ZrB_2–15 vol.%SiC and ZrB_2–30 vol.%SiC composites with smaller starting particle sizes in which the particle sizes of ZrB_2 and SiC are 2 μm and 0.5 μm, respectively, demonstrated marked plasticity and significant reduction in the flexural strength at 1800 °C. The flexural strengths of these two composites are 112 ± 12 MPa and 48 ± 10 MPa, respectively, and their corresponding strength retentions are 13% and 7%, respectively. Large ZrB_2 grains were commonly observed in the samples containing 15 vol.%SiC, which are always the sites for the crack initiation. Cavities were found in the samples containing 30 vol.%SiC and the grain boundaries are the main sites for the crack and cavity nucleation. To improve ultra-high temperature strength, larger starting particle sizes (ZrB_2 and SiC are 5 μm and 2 μm, respectively) were used for the preparation of ZrB_2–15 vol.%SiC. This sample fractured in an elastic manner up to 1800 °C and showed a very high strength with a value of 217 ± 16 MPa.

Keywords: B. Grain size; C. Fracture; C. Strength; D. Borides; D. SiC

1. Introduction

The high melting temperature of ultra-high temperature ceramics (UHTCs) makes them promising candidates for use in thermal protection systems (TPS) and propulsion systems in hypersonic aerospace vehicles.[1,2] Among the UHTCs, zirconium diboride (ZrB_2)-based ceramic composites have attracted much attention because of their unique combination of low density, high melting temperature and thermal shock resistance as well as excellent mechanical and chemical stability at high temperatures.[2–7]

Silicon carbide (SiC) is always added to ZrB_2 to improve the densification, oxidation resistance, fracture toughness and mechanical strength.[4,5,7–9] Recent studies of ZrB_2-based ceramic composites demonstrated that ZrB_2 with 15–30 vol.%SiC addition exhibited the good combination of strength, fracture toughness, and oxidation resistance.[3–5,9] SiC grain size has a strong influence on the densification microstructure and strength of ZrB_2–SiC ceramics.[9,10] Decreasing the average size of starting SiC particles enhanced the densification of ZrB_2–SiC, producing relative densities that increased from 97.4% to 99.8%, as the size of the SiC particles decreased from 10 μm to 0.45 μm. Both the ZrB_2 and SiC grain sizes in dense, hot pressed ceramics decreased as the size of the SiC decreased. The improvement of room temperature strength and oxidation resistance was attributed to the refinement of the microstructure.[10,11] Second phase additions reduce densification temperature and grain size, but the resulting ceramics may experience mechanical degradation at elevated temperature.[12] Hot-pressed ZrB_2-based composites show a significant loss of strength below 1500 °C which is well below temperatures expected in proposed applications (>1800 °C).[9,13,14] Typically, oxide impurities form grain boundary phases or become localized at triple grain junctions, which reduce strength.[15] Most of the recent investigations have been mainly focused on mechanical properties of these composites at room and high temperature and very little attention has been paid to flexural strength and fracture behavior of ZrB_2–SiC ceramic composites at ultra-high temperature.

The purpose of the paper is to report flexural strength and fracture behavior of ZrB_2 ceramic composites containing 15 vol.%SiC and 30 vol.%SiC at 1800 °C. The effects of the particles size and SiC content on the strength and fracture behavior were also discussed.

---

* Corresponding author. Tel.: +86 45186402382; fax: +86 45186402382.
E-mail address: huping@hit.edu.cn (P. Hu).

0955-2219/$ – see front matter © 2009 Elsevier Ltd. All rights reserved.
doi:10.1016/j.jeurceramsoc.2009.09.029

2. Experimental procedure

The samples used here for high temperature strength testing were fabricated from commercial ZrB_2 (Northwest Institute for Non-ferrous Metal Research, China) and SiC (Weifang Kaihua Micro-powder Co., Ltd., China) powders. The median particle sizes of ZrB_2 are 2 μm and 5 μm, respectively, and the median particle sizes of SiC are 0.5 μm and 2 μm, respectively. ZrB_2–15 vol.%SiC (ZS1) and ZrB_2–30 vol.%SiC (ZS2) composites with smaller starting particle sizes in which the particle sizes of ZrB_2 and SiC are 2 μm and 0.5 μm, respectively, were hot pressed at 1950 °C with an applied pressure of 30MPa. ZrB_2–15 vol.%SiC with larger starting particle sizes in which the particle sizes of ZrB_2 and SiC are 5 μm and 2 μm (ZS3), respectively, were hot pressed at 2000 °C with an applied pressure of 30 MPa.

Prior to the hot pressing, the powder batches were homogenized by wet mixing in ethanol using zirconia balls. All of the powder mixtures were dried by rotary evaporation at a temperature of 70 °C, a vacuum of 10 kPa, and a rotation speed of 120 rpm. The hot pressing cycles were carried out in argon atmosphere using a BN-coated graphite die. High temperature strengths were measured in three-point on 3.5 mm × 5 mm × 70 mm (thickness × width × length) test bars at 1800 °C. The span of tested samples is 60 mm and crosshead speed is 0.5 mm/min. For comparison, the room temperature flexural strength of these materials was also measured. Five specimens were tested for each experimental condition. The final densities were measured by the Archimedes method. The grain sizes were determined by intercept method measured from acid etched surfaces. Scanning electron microscopy (SEM; FEI Sirion, Holland) along with energy-dispersive spectroscopy (EDAX, USA) was used to characterize the composition and microstructure of the polished and fracture surfaces.

3. Results and discussion

Fully dense ZrB_2–SiC composites were obtained by hot pressing. The mean grain sizes of ZrB_2 in ZS1, ZS2 and ZS3 are about 4.5 μm, 3 μm and 8 μm, respectively. Corresponding grain sizes of SiC are about 1 μm, 1.5 μm and 3 μm, respectively. Obviously, the final grain sizes of ZrB_2–SiC composites were approximately proportional to starting powder size. Therefore, the effect of the particle size on the high temperature strength and fracture behavior can be explored based on these composites. Examination of room-temperature overload fracture surface of ZS3 revealed a fully transgranular mode of fracture, in which the fracture surface is very smooth. In contrast, the corresponding fracture surfaces of ZS1 and ZS2 demonstrated a transgranular/intergranular mode. The fracture mode of ZS3 changed into completely intergranular at 1800 °C suggesting that the strength of intracrystalline is higher than intergranular strength at this temperature. It is well known that both intergranular strength and transgranular strength decreased with increasing temperature and the former decreased more quickly than the latter. Thus, the fracture mode of the ZrB_2–SiC composites changed into fully intergranular mode. Moreover, the pull-out of SiC grains in ZS3 is obviously indicating the bonding strength of ZrB_2/SiC boundary at 1800 °C is lower in comparison to that of ZrB_2/ZrB_2 boundary.

Fig. 1. Macrographs of the samples after flexural testing at 1800 °C.

Fig. 1 shows the macrographs of the samples after flexural testing at 1800 °C. ZS3 samples exhibited a little deformation before fracture, whereas fracture did not occur for ZS1 and ZS2 after testing at this temperature even though undergone a large amount of deformation. Fig. 2 shows load–displacement curves of the flexural-strength tests at 1800 °C for ZrB_2–SiC composites. ZS1 and ZS2 exhibited marked plasticity while no plastic deformation before fracture was observed in the ZS3, with a load/displacement plot remaining completely linear. The flexural strengths of ZS1, ZS2 and ZS3 at 1800 °C are 112 ± 12 MPa, 48 ± 10 MPa and 217 ± 16 MPa, respectively, and their corresponding flexural strengths at room temperature are 865 ± 125 MPa, 705 ± 120 MPa and 500 ± 40 MPa, respectively. ZS3 exhibited the lowest strength at room temperature compared to the others. However, this composite showed a slight degradation in strength up to 1800 °C. Apparently, the absolute value of the flexural strength for ZS3 is higher than that of ZS1 and ZS2. Furthermore, ZS3 retained approximately 43% of the strength at room temperature, which is also much higher

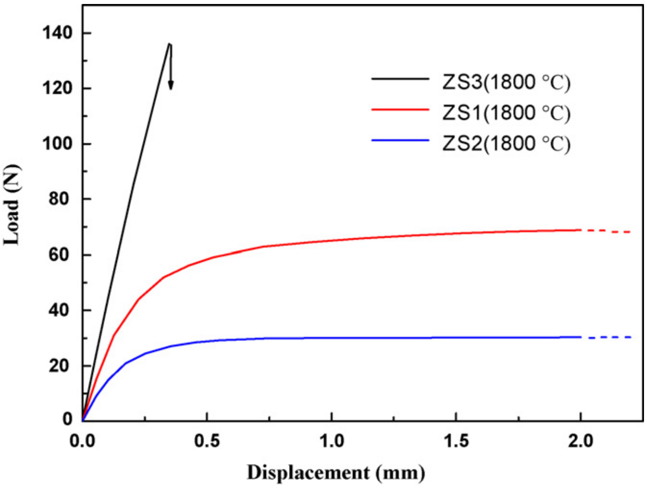

Fig. 2. Load–displacement curves as obtained from three-point bending experiments conducted at 1800 °C.

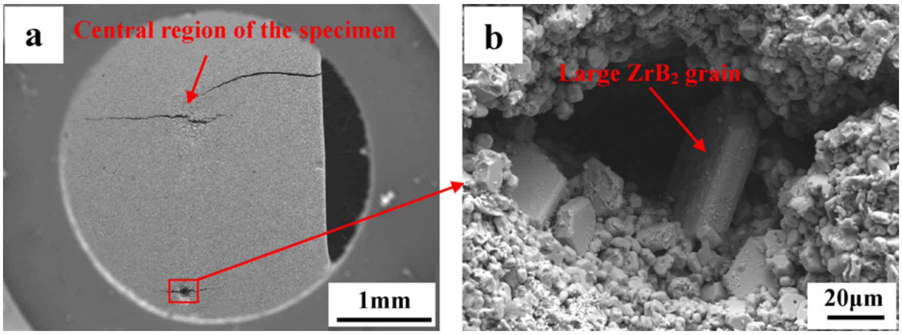

Fig. 3. SEM micrographs of the tensile side surface for ZS1.

than those of ZS1 (13%) and ZS2 (7%). Consequently, the flexural strength of ZrB_2–SiC ceramics at ultra-high temperature is strongly influenced by the grain size. Microstructural variations in ZrB_2–SiC composites often have opposing effects on room temperature strength and ultra-high temperature strength. Decreasing particle size is beneficial to the room temperature strength but detrimental to the ultra-high temperature strength. So, the tradeoff between room temperature and ultra-high temperature strength should be taken into account for applications. Comparison of the strengths of ZS1 and ZS2 revealed that high SiC content caused a significant reduction of the ultra-high temperature strength.

One striking observation in the ZrB_2–SiC specimens is that the fracture mode, crack formation and density are distinctly different from each other. ZrB_2–SiC ceramics consisted of coarser grains seem to be strong enough to prevent grain boundary sliding and induce fracture in an elastic manner, as previously described by the load–displacement curve in Fig. 2. Only one crack was detected in ZS3 specimen and no evidence of subcritical crack growth on the fracture surface was found. In contrast, several cracks were observed in ZS1 specimen (Figs. 3 and 4). The crack density remarkably increased in ZS2 (Fig. 5). Moreover, a large amount of cavities were also detected in ZS2 tested at 1800 °C.

Large ZrB_2 grains with a width of ∼50 μm were commonly observed in the samples with low SiC content because there is no enough SiC particles to effectively hinder exaggerated grain growth of individual ZrB_2 particle as a result of ZrB_2 particle agglomeration. The large grain region is always the site for the crack initiation as shown in Figs. 3 and 4. The stress easily builds up in the large particle region during deformation process leading to a lower threshold strain for the crack initiation, which ultimately induced the failure of the material. Consequently, the existence of individual large grain will significantly degrade the high temperature strength. Therefore, the control of the exaggerated growth of the individual grains becomes very important during the preparation of ZrB_2–SiC composites. However, this feature was not detected in ZrB_2–30 vol.%SiC composite due to the effective inhibition of exaggerated growth for ZrB_2 as a consequence of enough SiC particles. New cracks were formed ahead of the crack tip in ZS1 as can be seen in Fig. 4(a) resulting in the relaxation of the tensile stress intensity of the crack tip. Stress relaxation at the tensile region of the test specimens improved the stabilization of the cracks during high temperature deformation. Thus, the brittle fracture mode did not occur. ZS1 exhibited plastic deformation since crack propagation rate remarkably reduced as a consequence of crack thickening without significant growth. Cracks frequently nucleate at grain boundaries, especially at ZrB_2/SiC interface, and spread along the low angle boundaries (Fig. 6). ZrB_2 particles offer resistance to the further crack opening and propagation. Also, numerous microcracks parallel to the main crack were observed (Fig. 6(b)). The observation indicates that the strength of grain boundaries is lower than that of grains at 1800 °C and the decrease of the grain-boundary strength is responsible for the reduction of strength at elevated temperature. It has been reported that the existence of the low melting grain boundary phases will significantly decrease the high temperature strength due the softening of the grain boundary phases. HRTEM imaging showed that the amorphous films resulting from oxide impuri-

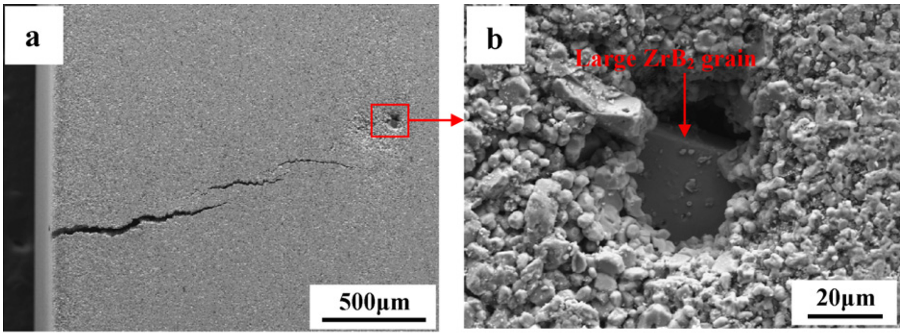

Fig. 4. SEM micrographs of the perpendicular tensile side surface for ZS1.

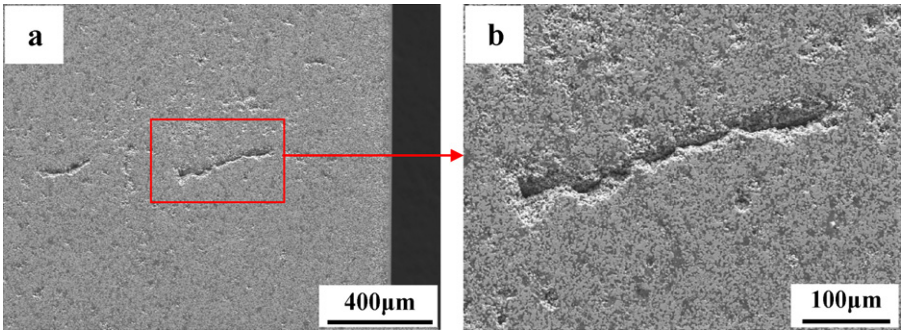

Fig. 5. SEM micrographs of the tensile side surface for ZS2.

ties existed at the part of the interphase interfaces, especially for the interphase interfaces between ZrB_2 and SiC.[11] The softening of these amorphous films would also account for a reduction of the grain-boundary strength. Therefore, the decrease in grain size and increase of SiC content would increase the frequency of the grain boundary phases leading to the degradation of the ultra-high temperature strength.

A large amount of cavities and cracks were detected at tensile side surface for ZS2 after flexural test at 1800 °C as indicated in Fig. 5. Cavities nucleated at random locations throughout the test specimen, eventually coalescing into cracks that were the source of failure at ultra-high temperature. The cracks have a low aspect ratio. Moreover, the strain to the crack and cavity formation of ZS2 is lower than ZS1. This result indicated that high SiC content containing UHTCs are less crack resistant than those with low SiC content. Examination of the cracks and cavities in the ZS2 revealed an intergranular fracture indicating that the grain boundaries are the main sites for the cavity nucleation. Such observations are consistent with published results on SiC that cavities were formed both at two-grain and multiple-grain junctions.[16] Moreover, there is no evidence of SiC particles in the cavity and crack region due to the spallation of SiC particles during high temperature deformation. In ZrB_2–SiC composites, there are three different types of grain boundaries i.e. ZrB_2/SiC, ZrB_2/ZrB_2 and SiC/SiC grain boundaries. Different sliding mobilities at ZrB_2/SiC, ZrB_2/ZrB_2 and SiC/SiC interface are expected to result in strain incompatibilities and thus cavitation. Due to the differences in chemical compositions and orientations, the sliding mobility for each combination is expected to be different. Therefore, the heterogenous interfaces are always the cavity nucleation sites. In the case of ZrB_2–SiC composites, ZrB_2/SiC interface is the dominant site for the cavity initiation. During the deformation process, it involves not only grain sliding but also grain rotation, which caused the spallation of SiC particles. This is why so much SiC particles have fallen out during high temperature flexural test. Talmy et al. invested the flexural creep deformation of ZrB_2–SiC ceramics in the temperature range of 1200–1500 °C and concluded that the SiC grain boundary sliding is the controlling creep mechanism in the ceramics containing 50 vol.%SiC.[17] Sato et al. studied the creep properties of Si_3N_4/SiC ceramics at 1250–1350 °C and reported that the creep deformation was controlled by grain boundary sliding accompanied by cavitation.[18] Grain boundary sliding and cavitation are the controlling deformation mechanism in ZS2 at ultra-high temperature.

For flexural specimen, it contained tensile and compressive regions. An examination of the perpendicular tensile side surface in ZS2 revealed the three different regions as can be seen in Fig. 7. This feature was not detected in ZS1 and ZS3. Note that the microstructure in tensile region is not the same. Spalling of SiC particles is obvious and the microstructure is relatively homogeneous and no large crack or cavity was detected in region (I), whereas a large amount of big cracks and cavities were observed beside spallation of SiC particles in region (II). This means extensive internal cavitation developed in the specimens. The consistent findings were reported by Fields and Wiederhorn.[19] In their studies, large cavities were also detected within the interior of the specimens. Such observations can be attributed to the condition of the applied load. The stress near the tensile side surface increases with increasing load and the spal-

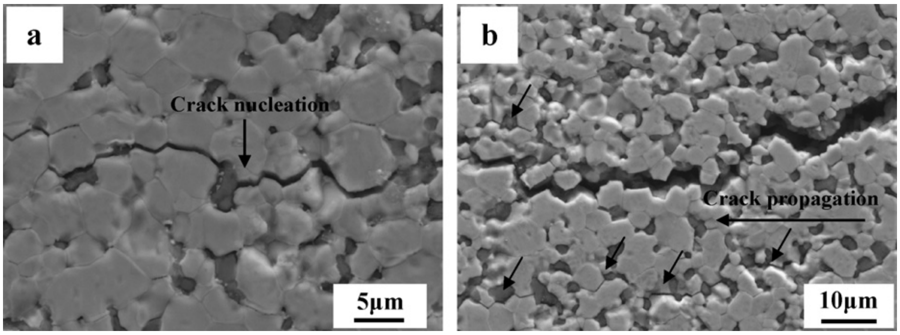

Fig. 6. Crack nucleation (a) and propagation (b) of ZS1. Numerous microcracks parallel to the main crack were formed as shown by arrows.

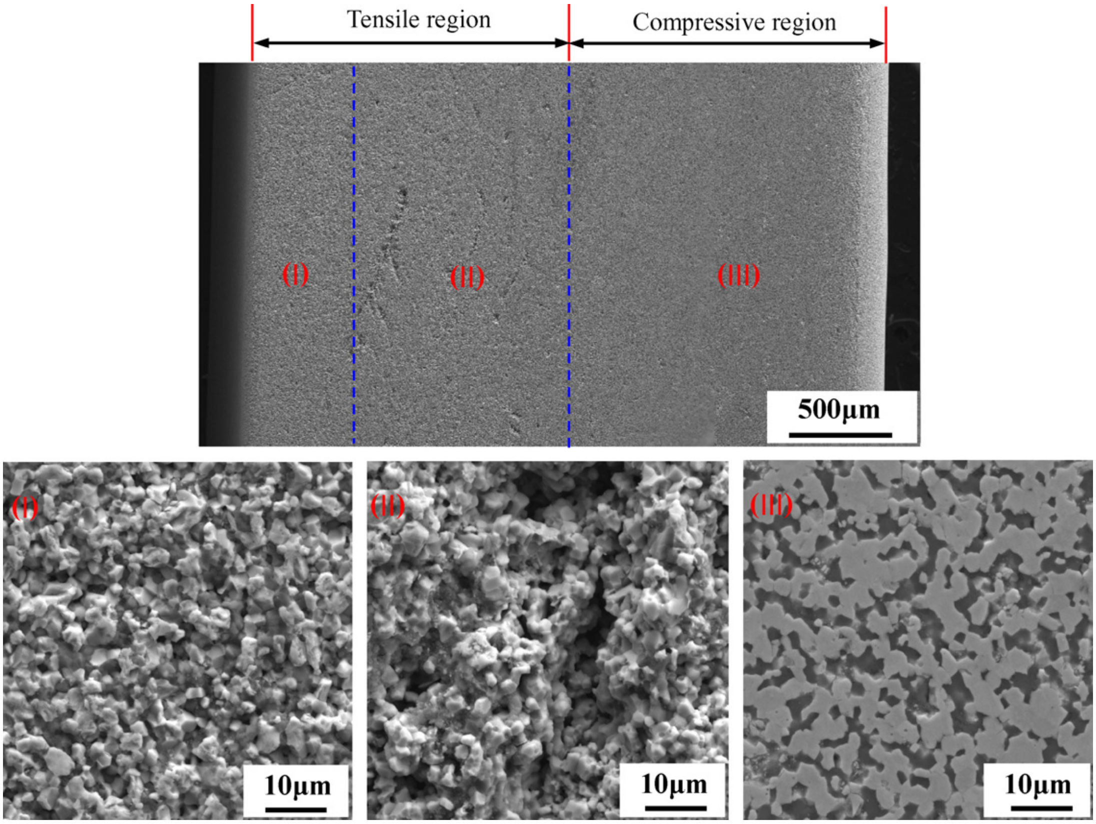

Fig. 7. SEM micrographs of the perpendicular tensile side surface for ZS2.

lation of single SiC particles, not a large area, would occur when it reaches the threshold stress for the breaking of the ZrB_2/SiC interface. The spallation of particles contributes to relaxation of the tensile stress and this would not cause the large area spallation. However, with further increased load the stress in region (II) is higher than threshold stress for crack initiation of both ZrB_2/SiC and ZrB_2/ZrB_2 interfaces and thus induces the large area failure. The cavity and crack growth was attributed to the debonding of the interfaces associated with spalling of SiC particles. It should noted that there is no change in the compressive region (III) and the microstructure of ZrB_2–SiC in this region is identical to the that of the material before flexural test.

4. Conclusions

The flexural strength and fracture behavior of the ZrB_2–SiC composites at ultra-high temperature significantly depends on the grain size and SiC content. ZrB_2–15 vol.%SiC and ZrB_2–30 vol.%SiC composites with finer grains demonstrated marked plasticity and did not fracture after flexural testing at 1800 °C, whereas ZrB_2–15 vol.%SiC with coarser grains fractured in an elastic manner without exhibiting plastic deformation up to 1800 °C and showed no evidence of subcritical crack growth on the fracture surface. The flexural strengths of ZS1 and ZS2 112 ± 12 MPa and 48 ± 10 MPa, respectively, and their corresponding strength retentions are 13% and 7%, respectively. Exaggerated growth of ZrB_2 grains were commonly observed in ZS1, which are always the sites for the crack initiation. Cavities were formed in the tensile region of the samples containing 30 vol.%SiC and the grain boundaries are the main sites for the crack and cavity nucleation. Grain boundary sliding and cavitation are the controlling flexural deformation mechanism in ZrB_2–30 vol.%SiC at ultra-high temperature. To improve ultra-high temperature strength, larger starting ZrB_2 (5 μm in size) and SiC (2 μm in size) particle sizes were used for the preparation of ZrB_2–15 vol.%SiC. The flexural strength of the composite at 1800 °C is 217 ± 16 MPa and the strength retention is 43%.

Acknowledgements

This work was supported by the National Natural Science Fund for Outstanding Youths (10725207), Postdoctoral Science Foundation of Heilongjiang province and Postdoctoral Science Foundation of China.

References

[1]. Upadhya, K., Yang, J. M. and Hoffman, W. P., Materials for ultrahigh temperature structural applications. *Am. Ceram. Bull.*, 1997, **72**(12), 51–56.
[2]. Opeka, M. M., Talmy, I. G. and Zaykoski, J. A., Oxidation-based materials selection for 2000 °C+ hypersonic aerosurfaces: theoretical considerations and historical experiences. *J. Mater. Sci.*, 2004, **39**, 5887–5904.
[3]. Chamberlain, A. L., Fahrenholtz, W. G., Hilmas, G. E. and Ellerby, D. T., High-strength zirconium diboride-based ceramics. *J. Am. Ceram. Soc.*, 2004, **87**, 1170–1172.
[4]. Han, W. B., Hu, P., Zhang, X. H., Han, J. C. and Meng, S. H., High-temperature oxidation at 1900 °C of ZrB_2–xSiC ultra-high temperature ceramic composites. *J. Am. Ceram. Soc.*, 2008, **91**(10), 3328–3334.

[5]. Zhang, X. H., Hu, P. and Han, J. C., Structure evolution of ZrB_2–SiC during the oxidation in air. *J. Mater. Res.*, 2008, **23**(7), 1961–1972.

[6]. Zimmermann, J. W., Hilmas, G. E. and Fahrenholtz, W. G., Thermal shock resistance of ZrB_2 and ZrB_2–30% SiC. *Mater. Chem. Phys.*, 2008, **112**, 140–145.

[7]. Monteverde, F., Bellosi, A. and Guicciardi, S., Processing and properties of zirconium diboride-based composites. *J. Eur. Ceram. Soc.*, 2002, **22**, 279–288.

[8]. Monteverde, F., Guicciardi, S. and Bellosi, A., Advances in microstructure and mechanical properties of zirconium diboride based ceramics. *Mater. Sci. Eng. A*, 2003, **346**, 310–319.

[9]. Monteverde, F., Beneficial effects of an ultra-fine α-SiC incorporation on the sinterability and mechanical properties of ZrB_2. *Appl. Phys. A*, 2006, **82**, 329–337.

[10]. Zhu, S., Fahrenholtz, W. G. and Hilmas, G. E., Influence of silicon carbide particle size on the microstructure and mechanical properties of zirconium diboride–silicon carbide ceramics. *J. Eur. Ceram. Soc.*, 2007, **27**, 2077–2083.

[11]. Hwang, S. S., Vasiliev, A. L. and Padture, N. P., Improved processing and oxidation-resistance of ZrB_2 ultra-high temperature ceramics containing SiC nanodispersoids. *Mater. Sci. Eng. A*, 2007, **464**, 216–224.

[12]. Melendez-Martinez, J. J., Dominguez-Rodriquez, A., Monteverde, F., Melandri, C. and Portu, G., Characterisation and high temperature mechanical properties of zirconium boride-based materials. *J. Eur. Ceram. Soc.*, 2002, **22**, 2543–2549.

[13]. Bellosi, A., Monteverde, F. and Sciti, D., Fast densification of ultra-high-temperature ceramics by spark plasma sintering. *Int. J. Appl. Ceram. Technol.*, 2006, **3**(1), 32–40.

[14]. Monteverde, F. and Bellosi, A., Development and characterization of metal-diboride-based composites toughened with ultra-fine SiC particulates. *Solid State Sci.*, 2005, **7**, 622–630.

[15]. Monteverde, F. and Bellosi, A., Efficacy of HfN as sintering aid in the manufacture of ultrahigh-temperature metal diborides–matrix ceramics. *J. Mater. Res.*, 2004, **19**(12), 3576–3585.

[16]. Chen, D., Sixta, M. E., Zhang, X. F., De Jonghe, L. C. and Ritchie, R. O., Role of the grain-boundary phase on the elevated-temperature strength, toughness, fatigue and creep resistance of silicon carbide sintered with Al, B and C. *Acta. Mater.*, 2000, **48**, 4599–4608.

[17]. Talmy, I. G., Zaykoski, J. A. and Martin, C. A., Flexural creep deformation of ZrB_2/SiC ceramics in oxidizing atmosphere. *J. Am. Ceram. Soc.*, 2008, **91**(5), 1441–1447.

[18]. Sato, S., Chu, M. C. K. Y. and Ando, K., Influence of SiC particle size on creep properties of Si_3N_4/SiC composite ceramics. *J. Ceram. Soc. Jpn.*, 1996, **104**(1215), 1035–1039.

[19]. Fields, B. A. and Wiederhorn, S. M., Creep cavitation in a siliconized silicon carbide tested in tension and flexure. *J. Am. Ceram. Soc.*, 1996, **79**(4), 977–986.